

WELDABILITY OF AUSTENITIC STAINLESS STEELS

S. L. Mannan* and V. Shankar**

*Associate Director, **Scientific Officer, Materials Development Group
IGCAR, Kalpakkam 603 102

Key Note :

Delivered at the Annual Seminar ('98-'99) Weld - '99 on Advances in Welding Technology, Calcutta July 9-10, 1999.

INTRODUCTION

Hot cracking is an important problem encountered during the welding of austenitic stainless steels. It is known that hot cracking occurs by the formation of low melting eutectic phases in the solidifying weld metal and in the heat-affected zone (HAZ), under the action of shrinkage stresses and restraint imposed on the joint (ref. 1-3). In the HAZ, cracking occurs by liquation of grain boundaries in the partially melted zone adjacent to the fusion line and in previously deposited weld metal in a multipass weld (ref.4). It has been found that cracking can be greatly reduced by selecting compositions that solidify in the ferritic mode (ref.5), or by reducing the concentration of impurity elements such as P, S, etc., to very low levels (ref.6,7). However, in the case of some materials such as fully austenitic stainless steels and nitrogen-bearing stainless steels, a primary ferritic solidification mode may not occur. In such cases, the levels of impurity and minor elements may critically determine the cracking behaviour.

In this work, the weld metal and HAZ cracking behaviour of one nitrogen-

bearing AISI 316LN and a fully austenitic Ti-stabilized 15 Cr-15Ni-2Mo stainless steel D9 (corresponding to ASTM A-771/UNS S38660) has been determined. The nitrogen-bearing stainless steel has gained importance because of their superior high-temperature properties and resistance to sensitisation over conventional AISI3161. The fully austenitic D9 alloy has been developed (ref.8) for use in core components of fast breeder reactors in view of its resistance to irradiation damage. These materials are candidates for use in the Indian fast breeder reactor program and it was essential to assess accurately their hot cracking susceptibility. A conventional Type 316L composition was also tested for comparison.

The addition of nitrogen is known to have a strong effect on weld microstructures (refs. 9-14). The delta-ferrite content decreases and the solidification mode changes from primary ferritic to primary austenitic, which necessitates a separate consideration of weldability in each solidification mode. In fully austenitic 18Cr-14Ni stainless steel, Kakhovski (13) and Zhitnikov (14) report beneficial effects of nitrogen addition up

to 0.2%. Similar results have been reported by Ogawa (9) and Lundin (12). Matsuda et al (11) found that in Type 304 weld metals, nitrogen addition increased the brittleness temperature range (BTR) to levels obtained in fully austenitic 310 material even when 1-3% delta-ferrite was present in the microstructure. They found enhanced phosphorus segregation with increase in nitrogen content. Nitrogen is also known to promote cracking in the weld metal HAZ (ref.15, 16), at locations where transformation of the delta-ferrite in the underlying weld bead takes place. A review of the weld metal cracking information therefore suggests that the correlation between composition and cracking would be greatly improved by considering nitrogen content along with the levels of impurities.

In fully austenitic materials such as alloy D9, the tolerable impurity levels for good weldability are generally low. Moreover, in Alloy D9, the presence of titanium increases the likelihood of fusion zone cracking as well as liquation cracking in the HAZ. Titanium is known to promote HAZ cracking in A286 and in Alloy 800 (refs.17,18), and optimum levels of

titanium depend on the carbon content. Titanium in excess of a Ti/C ratio of 5 is considered detrimental. On the other hand, certain minimum levels of elements such as Ti and P are desirable for irradiation swelling resistance. Hence, the composition of such a material must be optimised for good weldability. As information on the weldability of Alloy D9 is scarce, it was necessary to evaluate its cracking behaviour.

Evaluation of hot cracking susceptibility has traditionally employed several test methods, of which the Varestraint test in its several versions is widely used. The longitudinal Varestraint test (ref.19) has been extensively employed in the US, while the Transvarestraint test is preferred in Japan. The maximum crack length data from the Transvarestraint test has been used to derive the brittleness temperature

range on BTR, which is a material-specific parameter that enables comparison of materials weldability in a generalised way. Unlike in this test, the longitudinal test has largely been used to obtain a total crack length parameter that would vary with welding process and heat flow conditions. The suitability of these two test methods and their corresponding evaluation criteria have not so far been discussed in the literature.

This study therefore had as its objectives the following :

- Standardisation of the longitudinal Varestraint and Transvarestraint tests for measuring weldability in the fusion zone and HAZ.
- To investigate the influence of nitrogen content with particular reference to the levels of impurity elements on the hot cracking behaviour of type 316L weld metal.

- To examine the relation between composition and cracking in alloy D9. As part of a programme to evaluate weldability of reactor-grade stainless steels, studies were carried out on several heats of type 316L, 316LN and 304L stainless steels. The effect of nitrogen on weldability of 316L and 316LN was studied by addition of nitrogen to the shielding gas to obtain weld metal nitrogen contents in the range 0.04-0.2%. Three heats of D9 having Ti contents of 4,6 and 8 times the carbon level were tested. Type 321 and 347 steels were also tested for comparison.

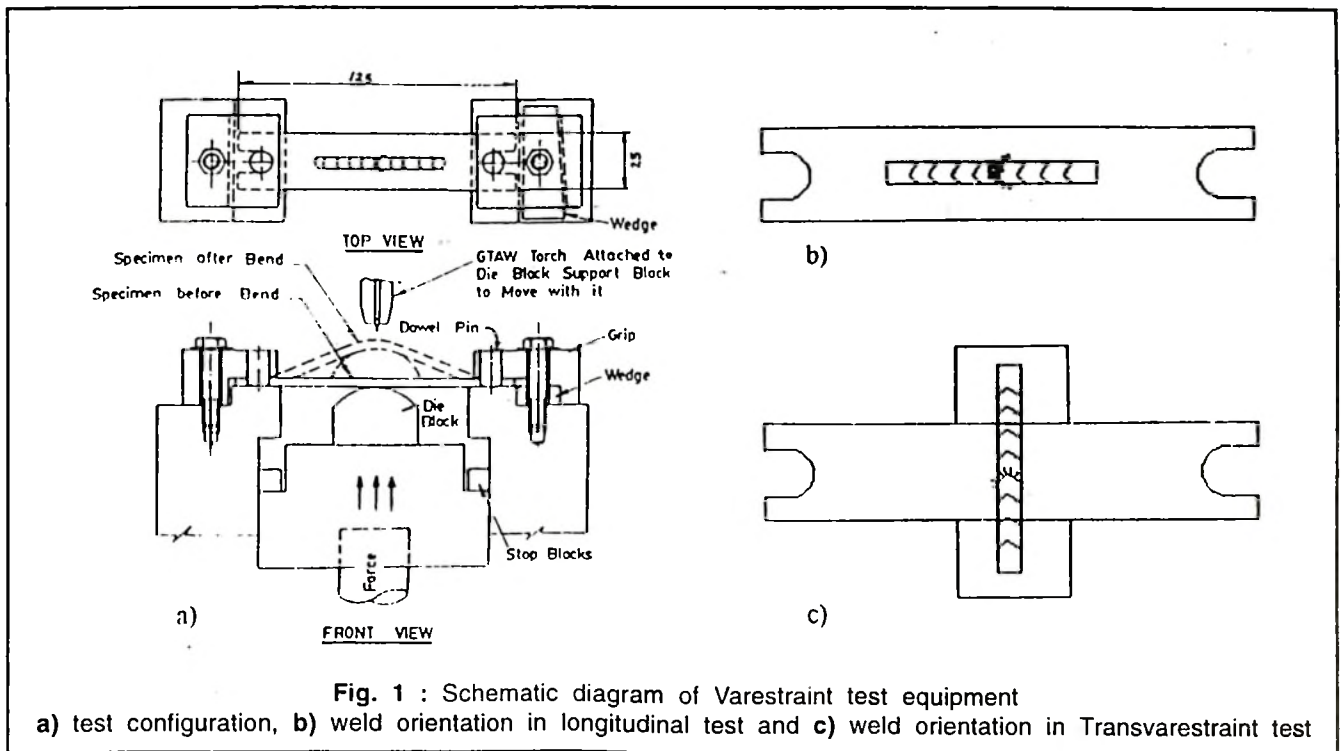
EXPERIMENTAL WORK

The compositions of the austenitic stainless steels used in this study are given in Table 1. The specimens were prepared from 3 mm thick sheet and tested using longitudinal and Transvarestraint tests. In the

Table 1 : Chemical Compositions of the Weld Metals Tested

Code	FN*	C	Mn	Cr	Ni	Si	Mo	N	P	S	Other
316LN	0.7 ¹	0.03	1.45	16.8	11.15	0.53	2.06	0.073	0.031	0.001	
316L	2.6 ²	0.029	1.8	17	11.9	0.7	2.25	0.036	0.035	0.012	
D9-A	0	0.052	1.5	15.1	15.04	0.5	2.26	0.011	0.011	0.002	0.21Ti
D9-B	0	0.051	1.5	15.05	15.06	0.5	2.25	0.011	0.011	0.002	0.32Ti
D9-C	0	0.052	1.5	15.11	15.26	0.52	2.26	0.011	0.012	0.002	0.42Ti
304L-A	0	0.016	1.51	18.12	11.58	0.53	-	0.039	0.023	0.018	
304L-B	3.0 ²	0.023	1.21	19.07	10.46	0.41	-	0.066	0.024	0.012	
304L-C	2.9 ²	0.023	1.67	18.88	10.09	0.42	-	0.069	0.031	0.019	
321	4.4 ²	0.051	1.88	17.6	9.9	0.68	-	0.009	0.038	0.012	0.33Ti
347	2.0 ¹	0.06	1.88	17.44	9.85	0.77	-	0.073	0.038	0.011	0.79Nb

* FN measured on Weld using Feritscope. Solidification modes : ¹-austenitic-ferritic (AF) ²-ferritic-austenitic (FA) the rest are fully austenitic (A)



longitudinal Varestraint test, a specimen of dimensions 127 x 25 x 3mm is welded along the length as shown in Fig. 1a and b. Strain is applied when the weld puddle reaches the middle of the specimen by bending rapidly over a ram of fixed radius. A 3-bead test technique was used to evaluate cracking in the fusion zone as well as HAZ (12). In this test, the straining is carried out pneumatically and is completed within 15 ms, so that the weld puddle is essentially 'frozen' at the instant of strain application. The strain experienced by the specimen is related to the radius of the die block by the relation $e = t/2R$ where e is the strain in the outer fibre, t the specimen thickness and R is the radius of the die block. In the Transvarestraint test (TVT), the weld bead is applied transverse to the specimen length (Fig. 1c). Run-on and run-off tabs are used so that

the weld bead is long enough to ensure thermal equilibrium at the instant of straining. Welding was carried out by GTAW process using welding conditions as shown in Table 2. During longitudinal Varestraint testing, the specimens generally showed conformity with the die blocks. However, during TVT, a greater tendency to kink at the weld bead was observed.

For evaluating the effect of nitrogen on cracking, nitrogen was added to the weld metal by mixing 0.25-5% N₂ through the shielding gas using a mass-flow control system of Bronkhorst make. Mixing was ensured by allowing the gases to pass through a manifold with suitable baffles.

The specimens were lightly pickled in an aqueous solution of nitric and hydrofluoric acids prior to crack

length measurement at 60x using a stereomicroscope. Ferrite was measured on the weld beads using a Fischer Feritscope model MP3-C. The ferrite contents and solidification modes are given in Table 1. Optical microscopy was carried out on the cracked specimens for detailed characterisation.

Table 2 : Welding Conditions and Specimen Thicknesses Used

Welding Conditions	
Current	: 100 A
Voltage	: 11 V
Welding Speed	: 4.2 mm/s
Electrode Dia	: 2.4 mm
Tip Angle	: 60°
Argon Flow	: 12 l/min

For deriving BTR from the maximum crack length, the centre line cooling curves of welds in all the materials were measured by plunging a 0.2 mm thick W-5%Re / W-26% Re thermocouple behind the arc using specimens and welding conditions identical to those in the actual tests. As the thermocouples were allowed to freeze into the weld metal, the temperature profile was captured using a HP data logger Model 34970A with a time resolution of 3 ms. A typical cooling curve for 316LN is shown in Fig.2. By calibrating the cooling curve in terms of distance using the welding speed, the temperature at the end of the crack was determined. The intersection of the liquid and solid state cooling curves was assumed to be the crack initiation temperature and the BTR values were calculated as the difference between this temperature and that of the crack tip.

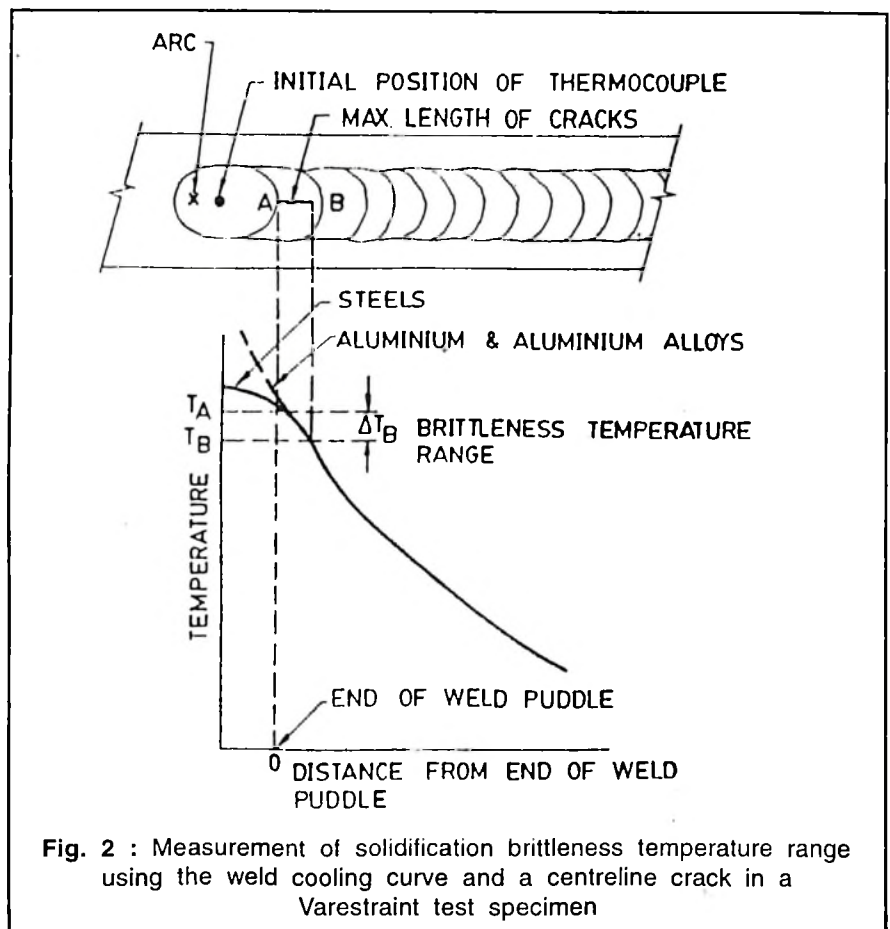


Fig. 2 : Measurement of solidification brittleness temperature range using the weld cooling curve and a centreline crack in a Varestraint test specimen

Metallography: After testing, crack lengths were measured on the specimens at 60X using a stereomicroscope. The cracked regions were cut and polished for metallographic observation after crack length measurements. The polished surfaces were etched electrolytically using either 10% oxalic acid or an aqueous solution of 55% orthophosphoric acid and 12% sulphuric acid before microscopic examination.

RESULTS AND DISCUSSION

Evaluation of Cracking :

The results of longitudinal Vareststraint and Transvareststraint tests are given in Figs. 3 to 6. Figs. 3(a) and (b)

show typical optical micrographs of cracking in type 347 specimens tested at 4% strain using both tests. In the LVT, the longest cracks were predominantly found away from the weld centre line (Fig. 3(a)), while most of the cracking occurred around the weld centre line in the TVT (Fig. 3(b)). The variation of TCL, with strain in the longitudinal test is shown in Fig. 4, where it is observed that the cracking increases with increasing strain in all cases. However, the materials solidifying in the austenitic mode (316LN, 304L-A, 347 and D9-A, B and C) show a sharp increase in cracking even at low strains, while the ferritic mode materials 316L, 321, 304L-B and C

show a threshold strain of 1-2% before appreciable cracking is observed. The MCL also increases with increasing strain.

The maximum crack length in the Transvareststraint test is shown as a function of strain in Fig. 6, where it is observed that the values are almost independent of strain for most of the compositions. That is, the MCL quickly reaches a value which remains nearly constant with increasing strain, except for the primary ferritic alloys 304L-B and C. This behaviour is unlike that in the LVT, where MCL continuously increases with strain. Here the Nb-bearing type 347 weld metal shows the highest cracking followed by the

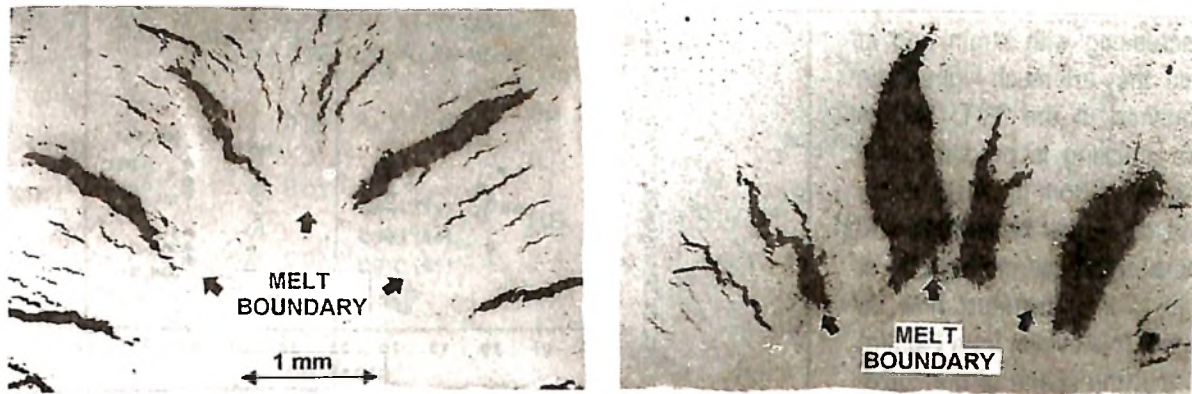


Fig. 3 : Typical appearance of cracking in a) Longitudinal Vareststraint specimen and b) Transvareststraint test specimen. Not the predominant centreline crack in Fig. 3b.

fully austenitic D9 heats, 316LN and 304L-A. The primary ferritic materials 316L, 304L-B and C exhibit the lowest values, the 304L-B and C showing a true cracking threshold of 2%.

The BTR values obtained using the TVT data are shown in Fig.7, where it is observed that all materials that had high TCL have BTR exceeding 40 C, while the primary ferritic materials show values less than 30 C. Using the longitudinal Vareststraint test, a material is considered crack-sensitive if the TCL values exceed 2.5 mm at 4% strain (12). Accordingly, the fully austenitic D9 and 304L-A, 316LN and the stabilized steels 347 and 321 are said to be crack-sensitive while the 316L, 304L-B and C would be considered crack-resistant. This behaviour is consistent with the solidification modes and levels of impurities present in the materials. It should also be noted that in the three D9 compositions, TCL increases by 30% while BTR increases by about 10°C when the Ti/C ratio is increased from 4 to 8.

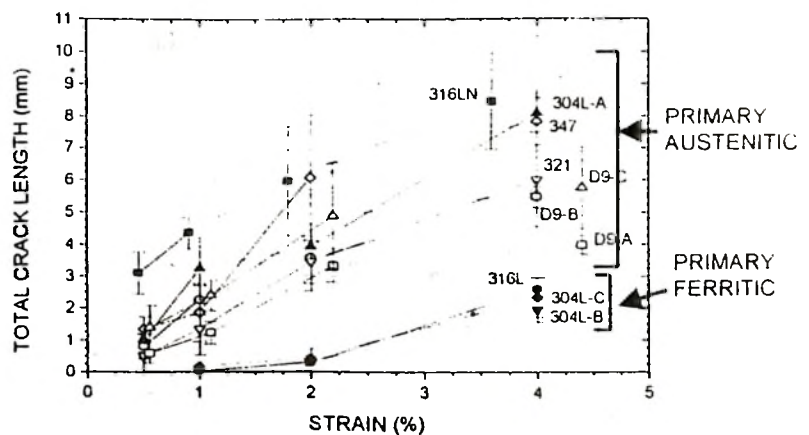


Fig. 4 : Variation of total crack length with strain in the Longitudinal Vareststraint Test

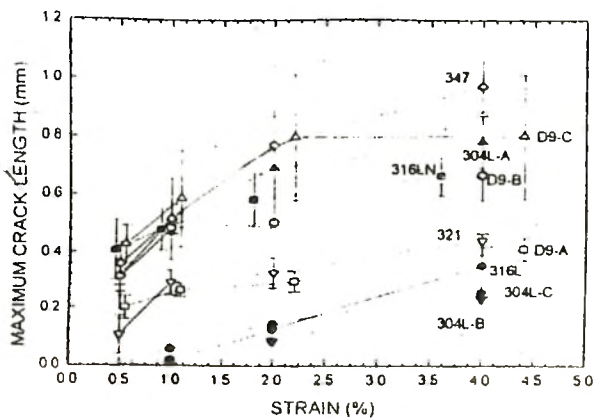


Fig. 5 : Variation of MCL with strain in the Longitudinal Vareststraint Test

A comparison of the MCL values shows that in the LVT the values keep increasing with strain and at 4% strain, they are much higher than that obtained in the TVT. This is because cracking is predominantly produced away from the weld centre line. The difference between centre line cracks and those propagating at an angle to this line must now be considered. It is evident from Fig.3(a) and (b) that the shape of the liquid-solid interface under consideration is elliptical. According to Garland and Davies (20), in an elliptically shaped weld puddle, the solid grains experience a continual change in the thermal gradient vector proceeding along the weld pool edge from the fusion boundary to the weld centre line. To keep up with this change in heat flow direction, grains 'bend' by dendrite side branching. Therefore, the grain boundaries are often curved and oriented away from the thermal axis at any instant. On the other hand, grain boundaries occur along the thermal vector at the weld centre, either because of impingement of grains from the base metal on either side. Since hot cracks propagate along grain boundaries, those located on the weld centre line would necessarily be aligned with the heat flow vector while those oriented at an angle would in most cases not be aligned with this vector and will be longer than the perpendicular distance between the ends of the crack. Hence, the distance between the isotherms at the crack tips, designated maximum crack distance or MCD was measured for all the materials and is shown in Fig. 8. It is observed that the data show

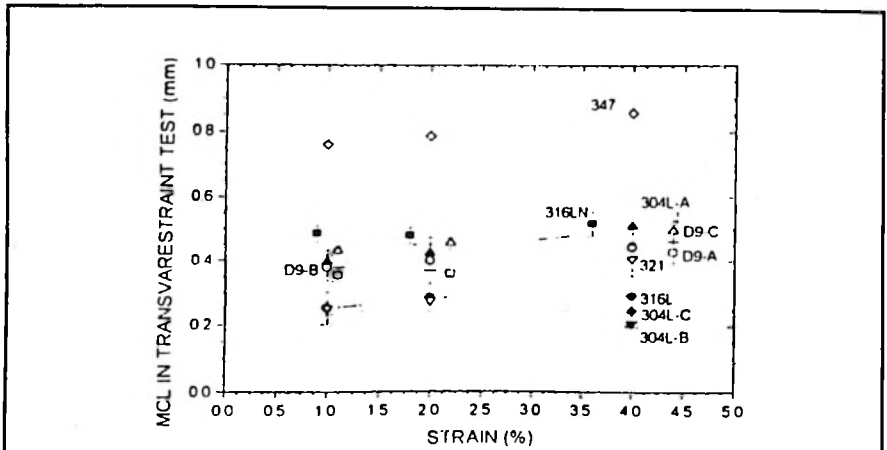


Fig. 6 : MCL in Transvarestraint Test as a function of strain

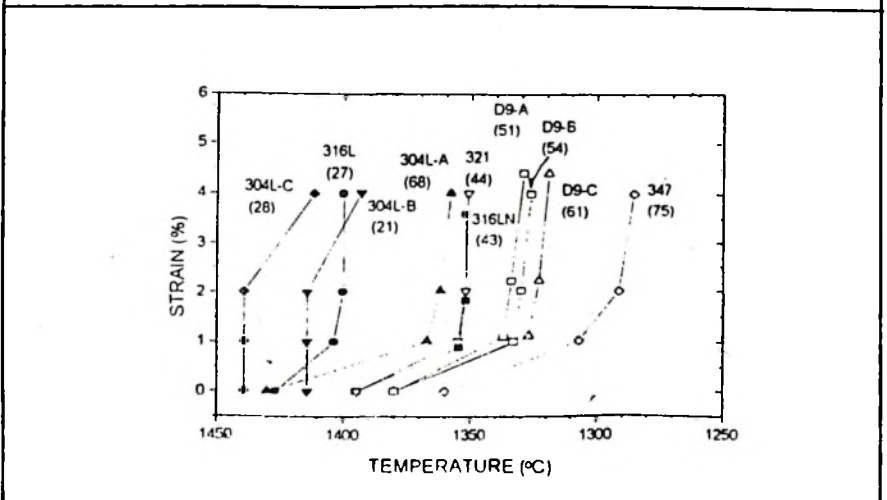


Fig. 7 : Brittleness temperature range vs. strain for the composition tested

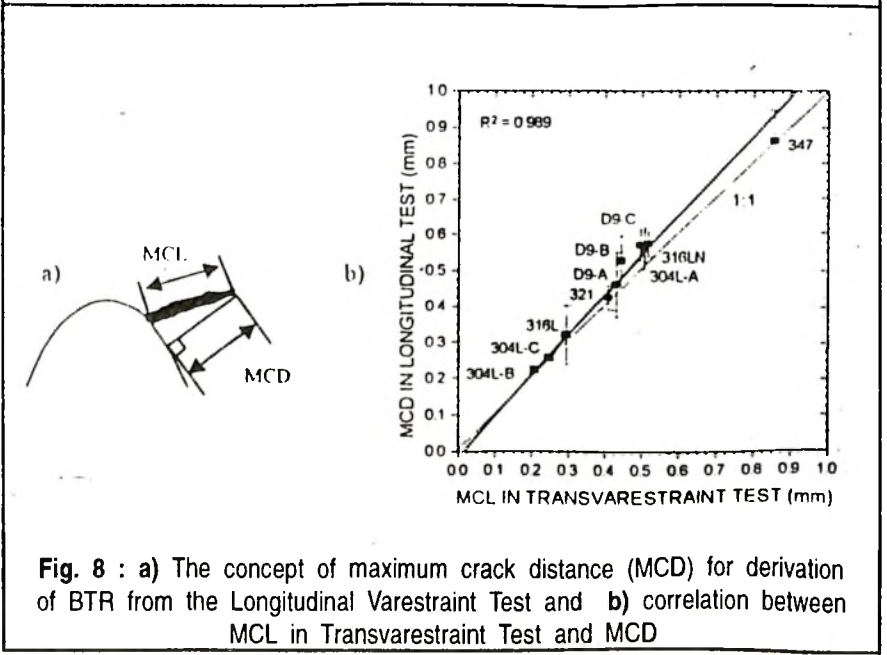


Fig. 8 : a) The concept of maximum crack distance (MCD) for derivation of BTR from the Longitudinal Vareststraint Test and b) correlation between MCL in Transvarestraint Test and MCD

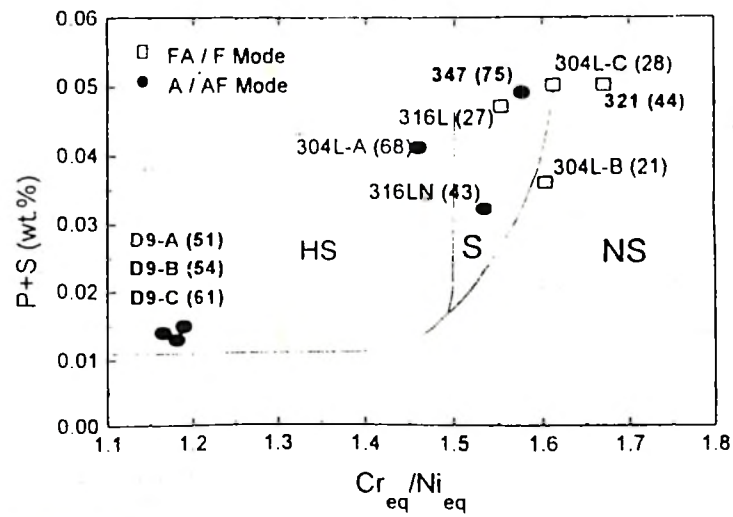


Fig. 9 : The hot cracking susceptibility of the weld metals tested represented on a map of Cr_{eq}/Ni_{eq} ratio vs P+S levels. HS, S and NS denote highly susceptible, susceptible and non-susceptible regions. Note that the stabilized stainless steels 321 and 347 do not follow the same trend as the unstabilized stainless steels.

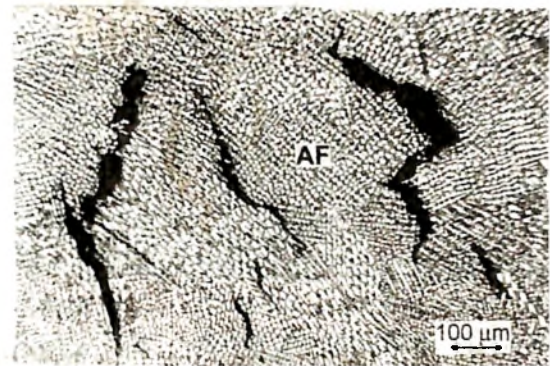
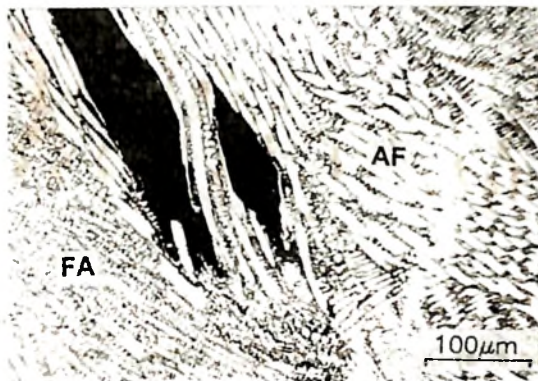


Fig. 10 : Microstructures showing fusion zone cracking in a) 316L and b) 316LN weld metal. Note cracking is confined to AF regions in 316L

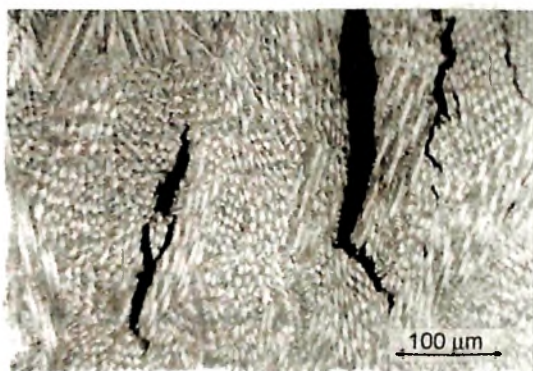


Fig. 11 : Microstructures of fusion zone cracking in stabilised stainless steels a) D9 showing cracks in A-mode microstructure and b) type 321 showing fine cracks in FA mode microstructure.

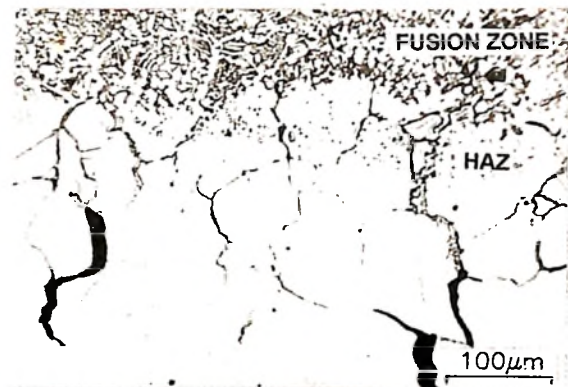
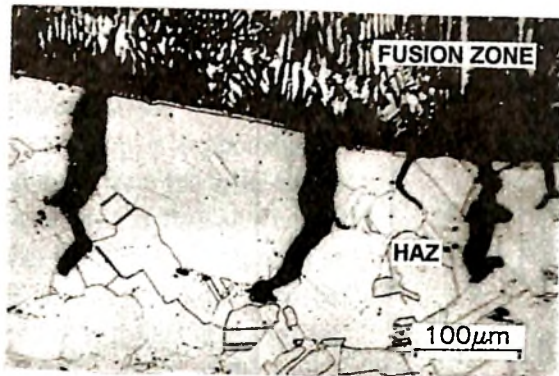


Fig. 12 : Micrographs of base metal HAZ cracking in a) 316L and b) 316LN. Note the extensive grain boundary melting observed in 316L and the associated wide partially melted zone in 316LN.

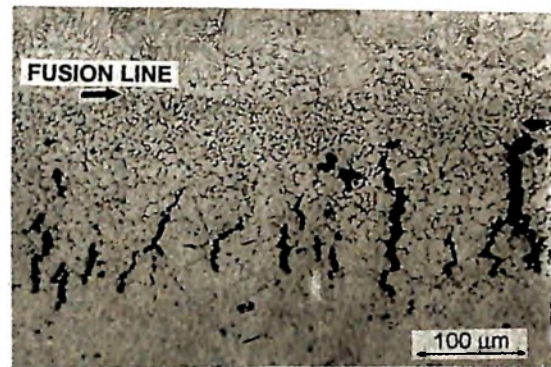
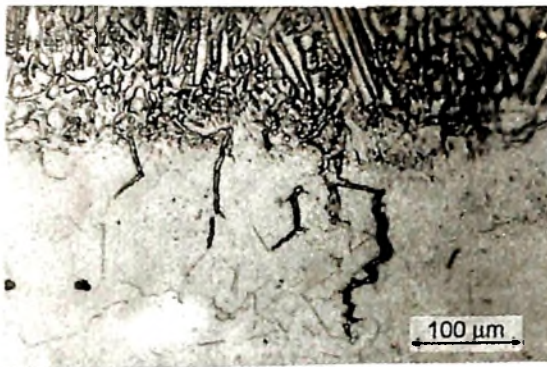


Fig. 13 : Photomicrographs of base metal HAZ cracking in a) D9 and b) type 321 stainless steel. Note the smaller width of cracking zone in type 321.

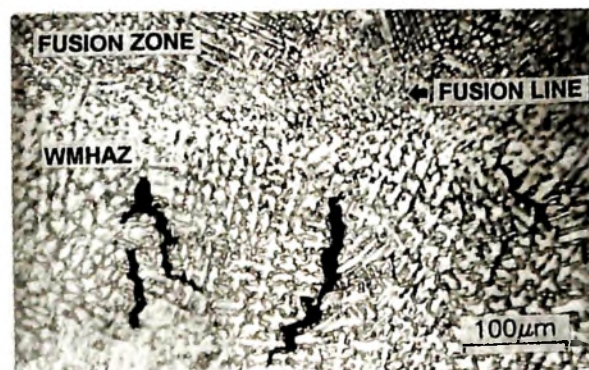


Fig. 14 : Weld metal HAZ cracking in type 316LN stainless steel

excellent correlation and nearly one-to-one correspondence between TVT-MCL and LVT-MCD. This clearly suggests that MCD provides a reasonable measure of BTR and can be used just as well as MCL from the Transvarestraint test to calculate this quantity (ref.21). The ability to calculate BTR using LVT results is important because this test can provide information on HAZ cracking in addition to solidification cracking in the same sample.

The correlation between composition and cracking in the materials tested is shown in Fig. 9, where the cracking is shown on a map of Cr_{eq}/Ni_{eq} ratio vs P+S content. This diagram, first used by Kujanpaa et al (22), is divided into three regions. For low Cr_{eq}/Ni_{eq} where the austenitic solidification mode occurs, alloys with P+S >0.011% are highly susceptible to cracking. Alloys solidifying as ferrite ($Cr_{eq}/Ni_{eq} > 1.5$), were not susceptible and could tolerate high levels of P+S without cracking. Lundin et al (12) showed that in the AF region where the ferrite content is limited, the cracking could be unacceptable if P+S is high and included an intermediate regime where the cracking tendency is a function of P+S level. The BTR values for the compositions tested do confirm the trend predicted by the diagram, except for 316LN, which shows higher cracking than 316L despite having a lower impurity level. This could possibly be due to enhanced segregation of P in the presence of N.

Microstructural Features of Cracking :

Fusion Zone Cracking : The microstructural features of fusion zone cracking observed in type 316L and 316LN are shown in Figs. 10a and b. Fig. 10a shows the cracking confined to AF regions in 316L that are arrested in a primary ferritic FA region. The primary austenitic 316LN shows extensive cracking (Fig.10b). Cracking in stabilized stainless steels D9 and 321 is shown in Fig. 11. The fully austenitic D9 shows many large cracks (Fig.11a) while the 321 showed a large number of fine cracks in an FA mode microstructure. The cracking was high despite the refinement in microstructure due to the presence of delta-ferrite. Extraction of segregated phases by electrochemical dissolution followed by X-ray diffraction analysis showed that D9 weld metal contained Ti_2CS , $Ti(C,N)$ and TiC phases in varying amounts (23). The proportion of $Ti(C,N)$ increased with increasing titanium content. This indicates that low melting eutectics containing these compounds are able to penetrate even the austenite ferrite boundaries that are usually resistant to wetting by phases containing P and S.

HAZ Cracking: Cracking in the base metal HAZ of 316L and 316LN are shown in Figs. 12a and b. Fig. 12a shows cracks in 316L. However, 316LN (Fig.12b) showed a much wider partially melted zone with extensive liquation of grain boundaries. Many cracks are also backfilled with liquid from the fusion zone. The higher cracking in 316LN is due to

the lower ferrite content that increases the susceptibility to cracking. In stabilized stainless steels, the HAZ cracking is generally much higher than in the unstabilized varieties. Fig. 13a and b show cracking in D9-B and type 321 weld metal respectively. The microstructure of D9 is fully austenitic while a primary ferritic structure with 4-5 FN is present in the 321. The D9 shows a wider crack-susceptible region, although the total amount of cracking is less. In 321, the width of the partially melted zone is observed to be smaller because of the higher ferrite potential.

Cracking in the HAZ of previously deposited weld metal (WMHAZ) of 316LN is shown in Fig.14. The cracking is more extensive in this region, since segregation is already present due to solidification. Further, the presence of an AF microstructure with a small amount of ferrite has been shown to be detrimental, since the ferrite in the underbead dissolves during the deposition of the subsequent pass to release harmful solutes such as P and S. Segregation of P has been previously shown to increase cracking in the WMHAZ(16).

Effect of Nitrogen on Cracking in 316L and 316LN :

The effect of nitrogen addition on hot cracking of type 316L and 316LN weld metals is shown in Fig.15. The initial microstructure of 316L was FA with some isolated regions of AF and a ferrite content of nearly 3 FN. As nitrogen content was increased from 0.036% to 0.07%, the FN decreased

to nearly 1 and the solidification mode was changed to AF. On further addition of nitrogen to 0.1-0.2%, there was a sharp increase in cracking by over 20%, which was retained at high levels of nitrogen up to 0.19%. However, a decrease in cracking tendency was observed for a nitrogen level of 0.12%. The increase in cracking due to nitrogen addition is explained by the increased segregation of P and S in the presence of nitrogen, which has been observed previously (24). However, in 316LN, quite an opposite trend was observed. Here, nitrogen addition over the initial level of 0.073% to 0.14 and 0.19% decreased the cracking by 25-30%, which is quite significant. The beneficial effect of nitrogen in 316LN is probably due to the grain refining tendency that has been attributed to nitrogen. However, a complete explanation of these results is still awaited.

CONCLUSIONS

1. Methodology for hot cracking testing of stainless steels was investigated using the longitudinal Varestreint and Transvarestreint tests. The results showed that the maximum crack distance (MCD) parameter obtained from the longitudinal test is equivalent to the MCL obtained using the Transvarestreint test. It was shown that brittleness temperature range for fusion zone cracking can be obtained from LVT.

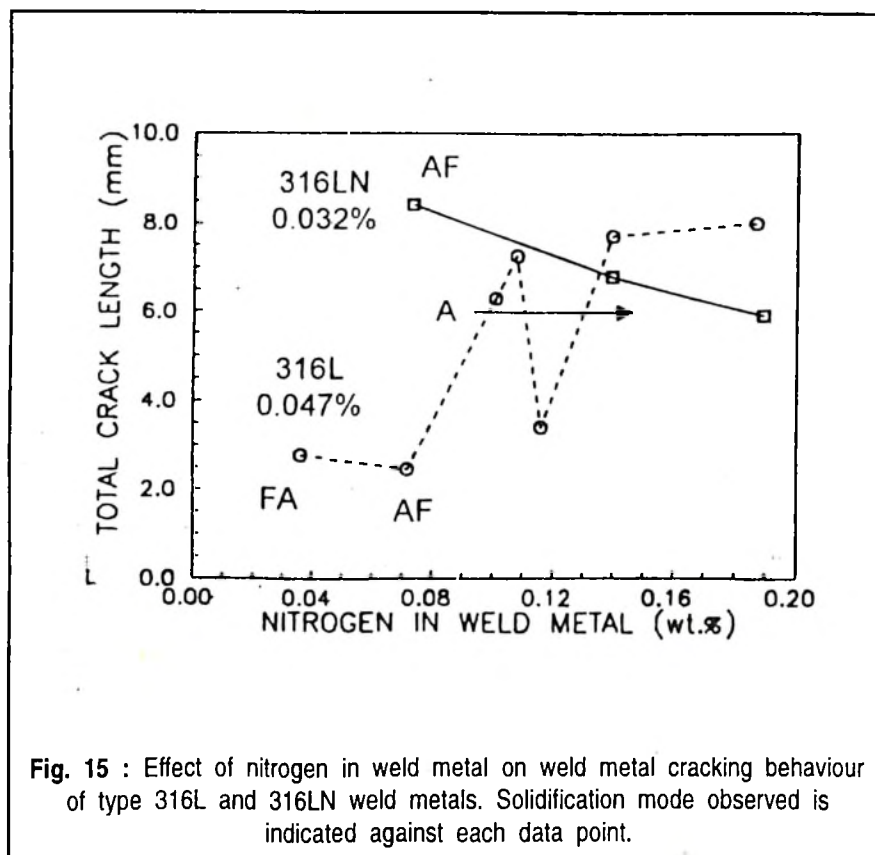


Fig. 15 : Effect of nitrogen in weld metal on weld metal cracking behaviour of type 316L and 316LN weld metals. Solidification mode observed is indicated against each data point.

2. Better correlation with composition was obtained using BTR criterion than with total crack length in LVT, according to the Suutala diagram. Stabilized stainless steels did not show reduced cracking with ferritic solidification mode and did not fit into the above correlation. This is probably due to the increased wetting of austenite-ferrite boundaries by liquid rich in solutes such as Ti, Nb in these steels.
3. Increasing Ti/C ratio from 4 to 6 caused an increase of cracking by 30% in alloy D9. The increased cracking was caused by the formation of greater amounts of Ti_2CS , $Ti(C,N)$ and TiC phases with increasing titanium content.
4. The effect of nitrogen on fusion zone cracking in austenitic-ferritic or austenitic weld metal was investigated. Nitrogen has a complex effect on fusion zone cracking that was dependent on the level of impurity elements P and S in type 316L weld metals. When the impurity level was low (0.032%), nitrogen addition upto 0.19% decreased cracking by up to 25% over the base level. However, at the higher impurity level N increased cracking significantly.
5. Microstructural examination of fusion zone and HAZ cracking

revealed that type 316LN weld metal showed more cracking and grain boundary liquation than 316L, despite having a lower impurity level. The stabilized stainless steels 321 and 347 showed a higher cracking tendency than unstabilized stainless steels. However, HAZ cracking in D9 alloys was low due to the lower impurity levels.

REFERENCES

1. Applett, W.R. and Pellini, W.S. 1954. Factors which influence weld hot cracking. *Welding Journal*. 33(2) : 83-s to 90-s.
2. Borland, J.C. 1960. Generalized theory of super-solidus cracking in welds (and castings). *British Welding Journal*, 7(8): 508-512.
3. Hull, F.C. 1960. Effects of alloying additions on hot cracking of austenitic stainless steels. *Trans. ASTM*. 60:667-690.
4. Lundin, C. D., DeLong, W.T. and Spond, D.F., 1975. Ferrite-fissuring relationships in austenitic stainless steel weld metals. *Welding Journal* 54(7):241-s to 246-s.
5. Masumoto, I, Takami, K and Kutsuna, M. 1972. Hot cracking of austenitic stainless steel weld metal. *Journal of the JWS*, 41(11):1306-1314.
6. Kujanpaa, V., Suutala, N., Takalo, T. and Moisio, T. 1979. Correlation between solidification cracking and microstructure in austenitic and austenitic-ferritic stainless steel welds. *Welding Research International*. 9(2):55-75.
7. Arata, Y., Matsuda, F., Nakagawa, H. and Katayama, S., 1978. Solidification crack susceptibility in weld metals of fully austenitic stainless steels (Report IV)-effect of decreasing P and S on solidification crack susceptibility of SUS 310 weld metals *Trans. Jap Weld. Res. Inst.* 7(2): 169-172.
8. Sundaram CV and Mannan SL 1989 *Sadhana*, 14 21-57.
9. Ogawa, T. and Tsunetomi, E. 1982 Hot cracking susceptibility of austenitic stainless steels. *Welding Journal* 61(3):82-s to 93-s.
10. Matsuda, F., Nakagawa, H., Katayama, S. and Arata, Y. 1983. Solidification crack susceptibility in weld metals of fully austenitic stainless steels (Report VIII) - Effect of nitrogen on cracking in SUS 304 weld metal. *Trans. JWRI* 12(1):89-95.
11. Ogawa, T., Suzuki, K. and Zaizen, T. 1984. The weldability of nitrogen-containing austenitic stainless steel: part II - porosity, cracking and creep properties. *Welding Journal* 63 (7):213-s to 223-s.
12. Lundin, C.D., Lee, C.H. and Qiao, C.Y.P. 1988. Group sponsored study--weldability and hot ductility behaviour of nuclear grade austenitic stainless steels. Final Report. Univ. of Tennessee. Knoxville, U.S.A.
13. *Kakhovskii N.I. et al. (1971) Effects of silicon, nitrogen and manganese on chemical heterogeneity in type OKh23N28M3D3T weld metals and their resistance to hot cracking. Avt. Svarka*, (8):11-14.
14. Zhitnikov N.P. 1981. *Welding Production* 28(3) pp 15-17.
15. Lundin, C.D. and Chou, C.P.D. 1985. Fissuring in the "hazard haz" region of austenitic stainless steel welds. *Welding Journal* 64(4): 113-s to 118-s.
16. Chou, C-P. D. and Wu, P-S., 1986. Effect of nitrogen on the austenitic stainless steel weld metal haz cracking. "Advances in Welding Science and Technology." ed., S.A. David. ASM, 703-707.
17. Lippold, J.C. 1983. An investigation of heat-affected zone hot cracking in Alloy 800. *Welding Journal* 62(1): 1-s to 11-s.
18. Brooks, J.A. 1974. Effect of alloy modifications on HAZ cracking of A-286 stainless steel. *Welding Journal* 53(11): 517-s to 523-s.
19. Lundin, C.D., Menon, R., Lee, C.H. and Osorio, V. 1985. New concepts in vareststraint testing for hot cracking in "Welding Research: The State of the Art" . JDC University Research Symposium Proceedings. ASM.
20. Davies, G.J. and Garland, J.G. 1975. *International Metals Reviews*, vol. 20, p83-106.
21. V. Shankar, T.P.S. Gill, S.L. Mannan and S. Sundaresan, 1999. "A Fundamental Investigation of Hot Cracking Evaluation Criteria using the Vareststraint Test," to appear in *Science and Technology of Welding and Joining*.
22. Kujanpaa, V., Suutala, N., Takalo, T. and Moisio, T. (1979) *Correlation between solidification cracking and microstructure in austenitic-ferritic stainless steel welds. Welding Research International* 9(2):55-76.
23. V. Shankar, T.P.S. Gill, S.L. Mannan and S. Sundaresan, 1999. unpublished work.
24. Brooks, J.A. (1975) Weldability of high N, high Mn austenitic stainless steel. *Welding Journal* 54(6): 189-s -195-s.